ELSEVIER

Journal of Power Sources 102 (2001) 135–138

JOURNAL OF POWER SOURCES

www.elsevier.com/locate/jpowsour

Electrode performance of romanechite for rechargeable lithium batteries

Masayuki Tsuda*, Hajime Arai, Yasue Nemoto, Yoji Sakurai

NTT Telecommunications Energy Laboratories, Tokai, Ibaraki 319-1193, Japan

Received 20 September 2000; received in revised form 20 December 2000; accepted 5 April 2001

Abstract

We studied romanechite, (2 × 3) tunnel type manganese dioxide, as a positive electrode material for rechargeable lithium batteries. We synthesized the sample by soft chemical techniques, and its chemical composition was $Ba_{0.18}MnO_{2.10}{\cdot}0.42H_2O$. We obtained a first discharge capacity of 120 mAh g^{-1} (energy density 264 mWh g^{-1}). The capacity decreased with cycling. We examined the thermal behavior of this material, revealing its high thermal stability. © 2001 Elsevier Science B.V. All rights reserved.

Keywords: Romanechite; Manganese dioxide; Soft chemistry; Positive electrode; Rechargeable lithium battery

1. Introduction

Manganese oxides have been intensively studied as a positive electrode material for rechargeable lithium batteries. Manganese oxides are less expensive, more widely available and generally have higher thermal stability than $LiCoO_2$ that is used in commercialized lithium ion batteries. Many groups have studied the lithium manganese spinel, $LiMn_2O_4$ [1,2]. The discharge curve of this spinel contains 3 and 4 V regions (vs. Li/Li^+). However, due to the limited cyclability in the 3 V region, only 4 V region is practically available and the energy density (480 mWh g^{-1}) is lower than that of $LiCoO_2$ (540 mWh g^{-1}).

Besides spinel $LiMn_2O_4$, there are many types of manganese dioxide with tunnel and layer structures. Their structural frameworks consist of MnO_6 octahedral units shared by corners and edges. Some have a large discharge capacity (typically 200 mAh g^{-1}) at the 3 V region and have recently been studied in detail. For example, Bach and Pereira-Ramos [3] have reported that hydrated layered manganese dioxide (birnessite) has a first discharge capacity of 200 mAh g^{-1}. Rossouw et al. [4] and Feng et al. [5] have reported the first discharge capacity of hollandite with a (2 × 2) tunnel structure to be 210 and 230 mAh g^{-1}, respectively. Lithiated manganese dioxide, $LiMnO_2$, has also been studied. This has two kinds of crystal structure. Layered α-$LiMnO_2$ (monoclinic) is synthesized from α-$NaMnO_2$ by ion exchange [6,7] while corrugated-layered β-$LiMnO_2$ (orthorhombic) is synthesized by the calcination of LiOH and γ-MnOOH [8]. Both have been reported to have large discharge capacities, but their cyclability is insufficient due to spinel transformation during cycling [6,9].

Here we report the electrode performance of romanechite, which has a one-dimensional (2 × 3) tunnel formed by corner and edge sharing MnO_6 octahedral units, as shown in Fig. 1. We expect romanechite to have a large capacity because it is structurally similar to hollandite. We also expect good cyclability because its large tunnel has the potential to accommodate lithium ions with little matrix distortion. To our knowledge there has been no report on the electrode performance of romanechite. We also report the thermal stability of romanechite.

2. Experimental

We synthesized romanechite according to the previously reported method [10]. This process uses soft chemical techniques, namely the ion exchange method followed by hydrothermal treatment. The precursor Na-birnessite (Na^+-form birnessite type manganese dioxide) was prepared as follows [11]. An amount of 250 ml of 5.5 M (mol dm^{-3}) NaOH solution was added to 200 ml of 0.5 M $MnCl_2$ solution at 10°C to form a white $Mn(OH)_2$ precipitate. We then bubbled oxygen into the $Mn(OH)_2$ precipitate at a rate 5 l min^{-1} for 5 h through a glass filter. After oxidation, the black Na-birnessite precipitate was filtered and washed with distilled water. Half the Na-birnessite was dispersed in 500 ml of 1 M $BaCl_2$ solution and stirred for 24 h at room

* Corresponding author. Tel.: +81-29-287-7683; fax:+81-29-287-7863.
E-mail address: tsuda@iba.iecl.ntt.co.jp (M. Tsuda).

PII: S0378-7753(01)00793-5

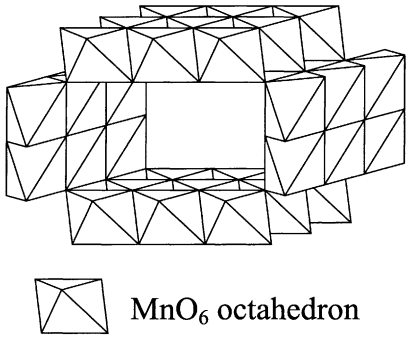

Fig. 1. Crystal structure of romanechite.

temperature to exchange Na^+ for Ba^{2+}. The product was filtered and washed with distilled water. We repeated this ion exchange treatment twice. Thus, prepared Ba^{2+}-exchanged birnessite (Ba-birnessite) was dispersed in 150 ml of 0.5 M $BaCl_2$ solution and hydrothermally treated at 180°C under autogeneous pressure. The hydrothermal treatment continued for 24 h unless otherwise stated. The sample was filtered, washed with distilled water and acetone, and then dried in air at 90°C.

We characterized the sample by X-ray diffraction (XRD) with Cu Kα radiation (Rigaku Rotaflex, Rint2000). We evaluated the chemical composition by using inductively coupled plasma emission (ICPE) spectroscopy and determined the manganese oxidation state by iodometry. We observed the morphology of the samples with a scanning electron microscope (SEM, Shimazu EPM-810). We observed the distribution of the elements (manganese, sodium and barium) on particles of the samples with an electron probe microanalyzer (EPMA, Nihondenshi JSM-5410).

We undertook electrochemical measurements using a coin cell with a metallic lithium negative electrode. The positive electrode mixture consisted of 70 wt.% of manganese dioxide, 25 wt.% of acetylene black as a conductive agent and 5 wt.% of polytetrafluoroethylene as a binder. The electrolyte was a 1 M $LiPF_6$ solution in equal volumes of ethylene carbonate and dimethyl carbonate. We started the measurement from discharge, with a cell voltage 2.0 ∼ 4.0 V and a current density 0.1 mA cm^{-2} at room temperature.

We measured the thermal behavior by using differential scanning calorimetry (DSC) combined with thermogravimetry (TG) to 700°C in an argon atmosphere.

3. Results and discussion

We assayed the obtained Na-birnessite, Ba-birnessite and romanechite samples in terms of their chemical compositions, morphology and distribution of elements. The evaluated chemical compositions of Na-birnessite and Ba-birnessite were $Na_{0.30}MnO_{1.95}\cdot 0.46H_2O$ and $Na_{0.04}Ba_{0.14}MnO_{1.99}\cdot 0.62H_2O$, respectively. This result shows that, during the ion exchange treatment, Na^+ was almost completely exchanged for Ba^{2+} while the manganese oxidation state was largely maintained. The chemical composition of the obtained romanechite was $Ba_{0.18}MnO_{2.10}\cdot 0.42H_2O$ and this composition is similar to $BaMn_5O_{10}\cdot H_2O$ ($Ba_{0.2}MnO_2\cdot 0.2H_2O$) reported by Joint Committee on Powder Diffraction Standards (JCPDS). Our romanechite sample had more hydrated water, but the water content seems to depend on the drying condition.

Fig. 2 shows the SEM images of the samples. The romanechite that we synthesized (Fig. 2(c)) was needle-like in form and this is quite unlike the hexagonal plate form of the precursors, Na-birnessite and Ba-birnessite (Fig. 2(a) and (b)). This result shows that the particle texture was maintained during the ion exchange whereas it was changed greatly by the hydrothermal treatment. The EPMA analysis indicated that sodium and barium were uniformly distributed on the particles of their respective samples, as was manganese. The equal distribution of the elements indicates the uniformity of the ion exchange and hydrothermal treatment without any phase segregation.

Fig. 3 shows the XRD pattern of the obtained romanechite sample. We also show the peak data for romanechite reported by JCPDS. Though our sample had lower crystallinity, we obtained romanechite as a single phase (Fig. 3(a)). This romanechite sample had a monoclinic unit cell, and its lattice parameters were $a = 14.0$ Å, $b = 2.48$ Å, $c = 9.79$ Å and $\beta = 92.4°$. We were not able to determine more precise values due to the low crystallinity of the sample, nevertheless, these values are close to those reported by JCPDS ($a = 13.94$ Å, $b = 2.846$ Å, $c = 9.683$ Å and $\beta = 92.32°$). We also conducted hydrothermal treatment for 48 h to obtain a sample with higher crystallinity. Fig. 3(b) shows the XRD pattern of this sample, confirming its higher crystallinity. However, the romanechite was partially transformed into Mn_3O_4 (indicated by arrows) by the longer hydrothermal treatment. Hereafter, we used the sample that had undergone 24 h of hydrothermal treatment.

Fig. 4 shows the discharge–charge profile of the romanechite sample we obtained. The first discharge profile indicates that most of the discharge region was below 3 V. We also observed this behavior for the second discharge and subsequent cycles. The first discharge capacity was 120 mAh g^{-1}, and the energy density was 264 mWh g^{-1} with an average voltage of 2.2 V. The capacity was smaller than other manganese dioxide compounds such as hollandite. The small capacity of the romanechite can be ascribed to the existence of Ba^{2+} tunnel ions. Although, the amount of Mn^{4+} available for reduction is 0.84 per manganese for the obtained romanechite $Ba_{0.18}MnO_{2.10}\cdot 0.42H_2O$, the existence of the heavy Ba^{2+} ions reduces the theoretical specific capacity of this sample to 186 mAh g^{-1}. The actual capacity was even smaller, possibly due to the ionic repulsion between Ba^{2+} and Li^+. Low crystallinity seems to be another reason for the small capacity. The first charge capacity (140 mAh g^{-1}) was larger than the first discharge

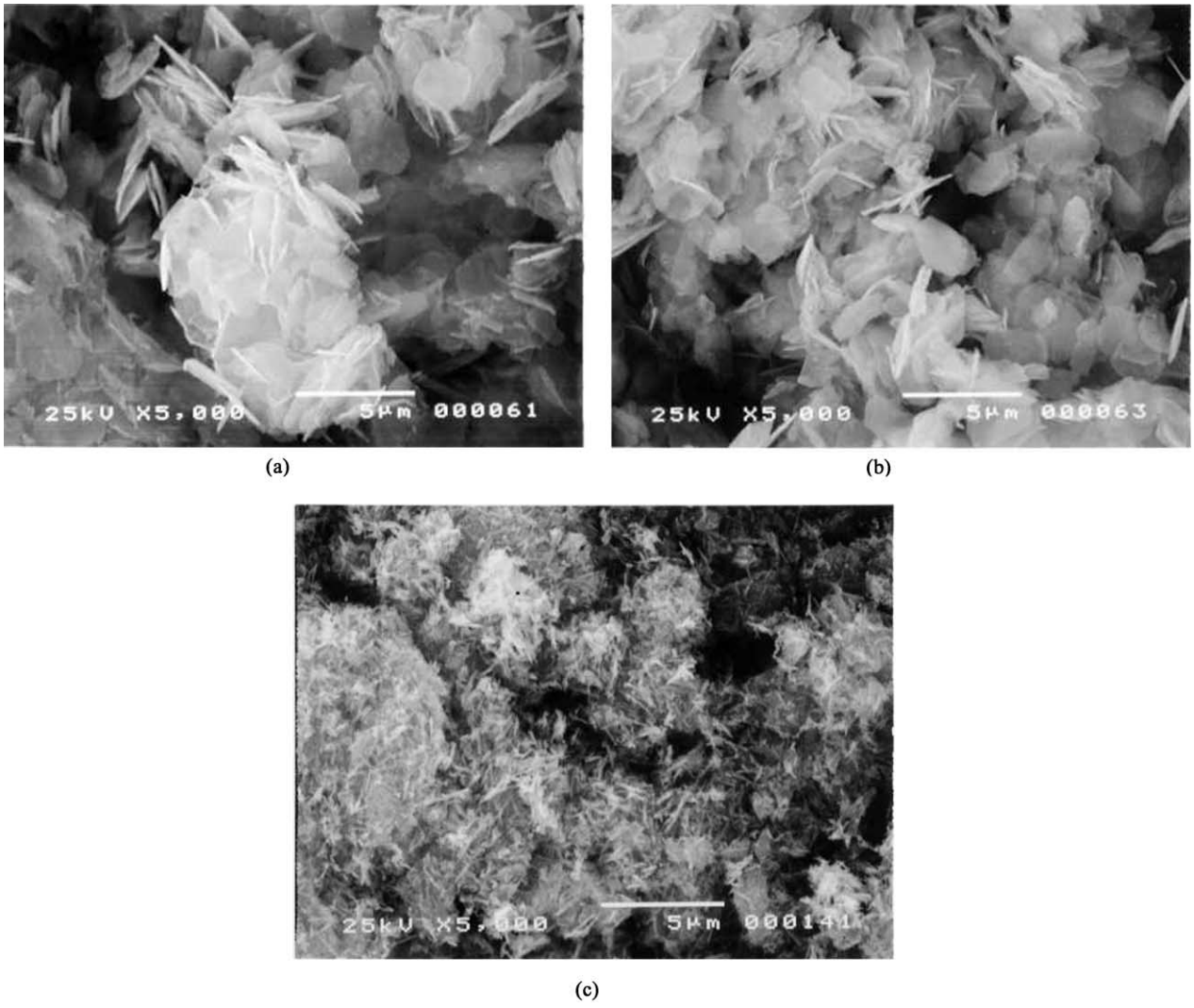

Fig. 2. SEM images of sample morphology: (a) Na-birnessite; (b) Ba-birnessite; (c) romanechite.

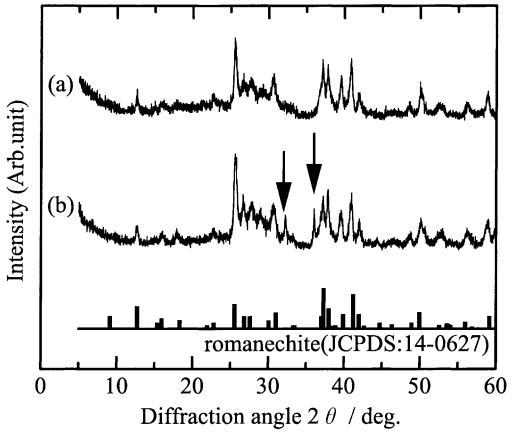

Fig. 3. XRD patterns of obtained romanechite: (a) 24 h; (b) 48 h hydrothermal treatment and peak data for romanechite from JCPDS. Arrows indicate peaks from by-product Mn_3O_4.

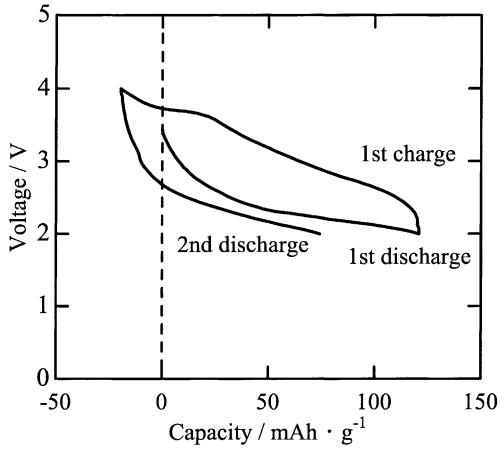

Fig. 4. Discharge–charge profile of obtained romanechite at 0.1 mA cm^{-2} between 2.0 and 4.0 V.

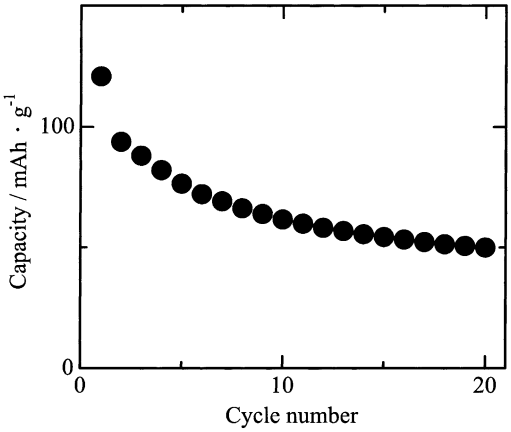

Fig. 5. Cyclability of obtained romanechite at 0.1 mA cm^{-2} between 2.0 and 4.0 V.

capacity. However, the second discharge capacity was 94 mAh g^{-1}, showing the poor reversibility of this material. As shown in Fig. 4 there was a voltage plateau at 3.7 V during charging that was not observed in the following discharge process. This suggests that the 3.7 V plateau corresponds to a side reaction and not to the lithium extraction. As large Ba^{2+} could hardly be extracted, water decomposition seems to be most probable.

Fig. 5 shows the cyclability of the obtained romanechite sample. There was a considerable capacity loss up to the fifth cycle. The capacity thereafter gradually decreased and was 50 mAh g^{-1} at the 20th cycle. During the initial five cycles, the charge capacity was larger than the discharge capacity and we observed a 3.7 V charging plateau. It is thus suggested that water decomposition hinders the lithium extraction, resulting in a large capacity loss. The XRD analysis indicated that the pristine romanechite structure was maintained after 20 discharge–charge cycles, but the crystallinity became low. Therefore, the capacity loss can be attributed to the partial matrix degradation due to the dehydration and also to the matrix distortion caused by the lithium insertion/extraction.

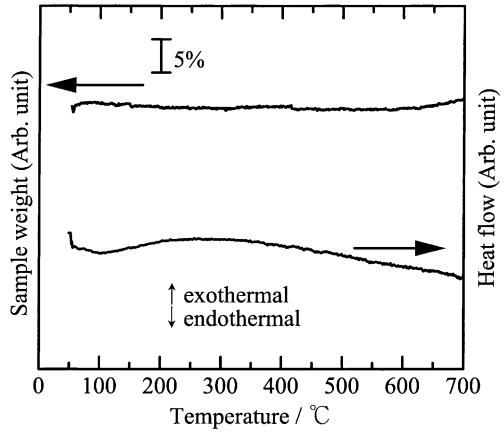

Fig. 6. TG–DSC profile of obtained romanechite in argon atmosphere at 10°C min^{-1}.

Fig. 6 shows the TG–DSC profile of the romanechite sample. The DSC curve contained no exothermal peak until 700°C, and we observed no notable weight increment or decrement in the TG curve. High temperature XRD analysis indicated that the romanechite structure was kept at least up to 500°C. The obtained romanechite sample is in the charged (delithiated) state, which is generally less stable than the discharged (lithiated) state. Nevertheless, it has high thermal stability, suggesting that the battery containing the romanechite electrode shows high safety standards. The high temperature XRD also showed that romanechite was transformed into hollandite at temperatures between 500 and 600°C, though we observed no noticeable exothermal or endothermal behavior in the DSC measurement. This may be due to the structural similarity between romanechite and hollandite.

4. Conclusion

Romanechite functions as a positive electrode material for rechargeable lithium batteries. Its single phase $Ba_{0.18}MnO_{2.10}{\cdot}0.42H_2O$ is obtained by ion exchange from Na-birnessite to Ba-birnessite followed by hydrothermal treatment at 180°C for 24 h. It has a first discharge capacity of 120 mAh g^{-1}. Exchanging the heavy Ba^{2+} for lighter ions could enlarge this capacity. The cyclability is poor and needs to be improved. Moreover, romanechite maintains its structure up to 500°C, showing its high thermal stability.

Acknowledgements

The authors express their gratitude to Mr. Kazuhiko Komatsu and Dr. Ichiro Yamada for their encouragement during the course of this research. The authors are also grateful to Ms. Noriko Kurusu and Mr. Ryuichi Nishio (both of NTT Advanced Technology) for their excellent technical support.

References

[1] M.M. Thackeray, P.J. Johnson, L.A. de Picciotto, Mater. Res. Bull. 19 (1984) 179.
[2] T. Ohzuku, M. Kitagawa, T. Hirai, J. Electrochem. Soc. 137 (1990) 769.
[3] S. Bach, J.P. Pereira-Ramos, J. Electrochem. Soc. 143 (1996) 3429.
[4] M.H. Rossouw, D.C. Liles, M.M. Thackeray, Mater. Res. Bull. 27 (1992) 221.
[5] Q. Feng, H. Kanoh, K. Ooi, M. Tani, Y. Nakacho, J. Electrochem. Soc. 141 (1994) L135.
[6] A.R. Armstrong, P.G. Bruce, Nature 381 (1996) 499.
[7] F. Captaine, P. Gravereau, C. Delmas, Solid State Ionics 89 (1996) 197.
[8] T. Ohzuku, A. Ueda, T. Hirai, Chem. Express 7 (1992) 193.
[9] R.J. Gummow, D.C. Liles, M.M. Thackeray, Mater. Res. Bull. 28 (1993) 1249.
[10] Q. Feng, K. Yanagisawa, N. Yamasaki, Solvothermal React. 2 (1996) 264.
[11] D.C. Golden, J.B. Dixon, C.C. Chen, Clays Clay Minerals 34 (1986) 511.